

# Studies of inclusion complexes of natural and modified cyclodextrin with (+)catechin by NMR and molecular modeling

Carolina Jullian,<sup>a,\*</sup> Sebastián Miranda,<sup>b</sup> Gerald Zapata-Torres,<sup>b</sup> Fernando Mendizábal<sup>c</sup> and Claudio Olea-Azar<sup>b</sup>

<sup>a</sup>Departamento de Química Orgánica y Físicoquímica, Facultad de Ciencias Químicas y Farmacéuticas, Universidad de Chile, Casilla 233, Santiago 1, Chile

<sup>b</sup>Departamento de Química Inorgánica y Analítica, Facultad de Ciencias Químicas y Farmacéuticas, Universidad de Chile, Casilla 233, Santiago 1, Chile

<sup>c</sup>Departamento de Química, Facultad de Ciencias, Universidad de Chile, Casilla 653, Santiago, Chile

**Abstract**—The aim of this paper is to describe the inclusion properties and the factors affecting the complexation selectivity and stabilization of catechin (CA) into  $\beta$ -cyclodextrin ( $\beta$ -CD) and two of its derivatives, namely Heptakis 2,6-di-*O*-methyl- $\beta$ -cyclodextrin (DM- $\beta$ -CD) and 2 hydroxypropyl- $\beta$ -cyclodextrin (HP- $\beta$ -CD). Analysis of the proton shift change using the continuous variation method confirm the formation of a 1:1 stoichiometric complex for catechin and the different CDs in aqueous medium. The formations constant obtained by diffusion-ordered spectroscopy (DOSY) techniques indicated the following trend upon complex formation:  $\beta$ -CD > HP- $\beta$ -CD > DM- $\beta$ -CD. The detailed spatial configuration is proposed based on 2D NMR methods. These results are further interpreted using molecular modeling studies. The latter results are in good agreement with the experimental data. The models confirm that when CA- $\beta$ -CD is formed, the catechol moiety in the complex is oriented toward the primary rim; however when CD is derivatized to HP- $\beta$ -CD and DM- $\beta$ -CD this ring is oriented toward the secondary rim.

## 1. Introduction

Catechins are phenolic compounds extracted from plants and present in natural food and drinks, such as green tea<sup>1</sup> or red wine<sup>2</sup> (Fig. 1). The role of such molecules in the prevention of cancer and cardiovascular diseases has received a great deal of attention.<sup>3,4</sup> Catechins are scavengers of reactive oxygen species, and their resulting anti-oxidant properties are of great interest in dietetics and cosmetology. Furthermore, their antiviral and cancer inhibiting properties could have pharmaceutical applications.<sup>5</sup> However, catechin powders are bitter, brown, and easily get oxidized, and hence difficult to use as a natural food additive or medicine.

Cyclodextrins are cyclic oligosaccharides composed of glucopyranose units and can be represented as a truncated cone structure with a hydrophobic cavity. Their most popular feature is the marked difference of polarity

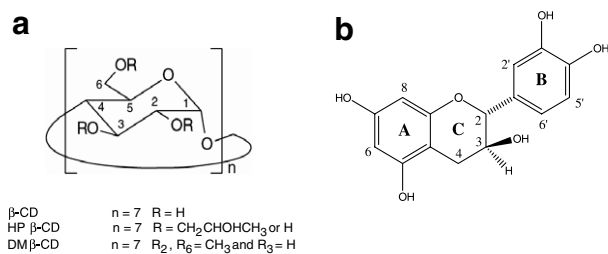


**Figure 1.** Molecular structures of  $\beta$ -cyclodextrin, 2-hydroxypropyl- $\beta$ -cyclodextrin, and Heptakis-2,6-*O*-di-methyl- $\beta$ -cyclodextrin (a). Molecular structure of (+)catechin (b).

between the internal and external surfaces: the inner part is made apolar by the glycosidic oxygens and methine protons, whereas the external surface is polar by virtue of the presence of secondary and primary hydroxyls on the large and small rims, respectively, thus allowing their solubilization in water. These unique properties predispose them to form inclusion complexes, as the displacement of included water molecules by apolar substrates represents a thermodynamically favored

**Keywords:** (+)Catechin; Cyclodextrin; NMR; Molecular modeling.

\* Corresponding author. E-mail: cjullian@uchile.cl

process.<sup>6</sup> In the pharmaceutical, cosmetics, and food industries, cyclodextrins have been used primarily as complexing agents to increase the water solubility of various compounds, such as drugs, vitamins, and food colorants.<sup>7</sup> It was demonstrated that complexation can considerably increase the stability and bioavailability of the guest molecules. We have recently reported the enhancement in solubility of flavonoid (quercetin and morin) through phase solubility experiments in different cyclodextrins.<sup>8,9</sup>

This work describes the result obtained from nuclear magnetic resonance (NMR) studies on the inclusion properties of CA into  $\beta$ -cyclodextrin and two derivatized cyclodextrins, Heptakis-2,6-di-*O*- $\beta$ -cyclodextrin (DM- $\beta$ -CD) and 2-hydroxypropyl- $\beta$ -cyclodextrin (HP- $\beta$ -CD). We observed the possible factors that affect the complexation selectivity and stabilization. The formation constant are obtained by diffusion-ordered spectroscopy (DOSY) techniques, while the detailed spatial configuration is proposed by 2D NMR. We also carried out molecular modeling studies to build three-dimensional models of substituted and native  $\beta$ -CD upon complexation with CA in order to provide a more detailed description of the interactions so as to rationalize the experimental results.

## 2. Results and discussion

### 2.1. <sup>1</sup>H NMR studies

<sup>1</sup>H NMR data for CA dissolved in D<sub>2</sub>O show well-resolved signals in two distinct spectral regions: two doublets corresponding to methylene protons, H-4, and a multiplet centered at 4.16 ppm due to the methine nuclei H-3, which are *J*-coupled to the adjacent methylene protons H-4 and to the methine H-2 (however the signal of the latter is not being observed because it is superimposed with the water signal at 4.7 ppm). In the high frequency region, the two-spin system and the three-spin system of ring A and B, respectively, are clearly detected (Fig. 2).

The formation of inclusion complexes can be proved from the changes of chemical shifts of CA or CDs in <sup>1</sup>H NMR spectra. Figure 3 illustrates that most of the aromatic protons of CA are influenced owing to the presence of CDs. Table 1 lists the detailed variation of the aromatic chemical shifts of CA before and after forming inclusion complexes with CDs. Upfield shifts are observed for all the aromatic protons of the A- and B-rings. However, the major induced shielding is observed for all the B-ring protons on both CA- $\beta$ -CD and CA-DM- $\beta$ -CD complexes. But it is worth to mention that the H-8 A-ring proton in the DM- $\beta$ -CD complex shows outstanding upfield chemical shifts in comparison with the other complex. The broadening of the proton signals of CA in the presence of CD suggests that the B-ring, the C-ring, and the A-ring are included in the cavity and hence the motions of these protons are restricted indicating that CA molecule fitted tightly.<sup>10</sup>

The H-3 and H-5 protons of the glucose units are facing to the interior of the CD cavity, whereas H-6 protons are located at the rim with the primary alcohols. H-2 and H-4 are at the opposite entrance of the cavity. Upfield shifts of the interior proton signals of CDs are indicative that aromatic guest molecules are located close to the protons for which a shift is observed. This displacement is due to the anisotropic magnetic effect induced by the presence of the aromatic group of the guest molecule. The analysis of the variations undergone by CDs protons as a consequence of the presence of CA strongly suggests complexation involving inclusion into the cavity of the host, as the external protons H-1, H-2, and H-4 were slightly affected, whereas the H-3, H-5, and H-6 protons were significantly shifted (data not shown).

One important NMR application is the association constant determination ( $K_a$ ) for host-guest complexes using <sup>1</sup>H chemical shift information.<sup>11</sup> Recently there has been a growing interest in the use of pulsed field gradient methods to provide information on  $K_a$  via the molecular self-diffusion coefficient.<sup>12,13</sup> The diffusion coefficient ( $D$ ) depends on the size of the molecule:

$$D = \frac{kT}{6\pi\eta r} \quad (1)$$

where  $k$  is the Boltzmann constant,  $T$  is the absolute temperature,  $\eta$  is the dynamic viscosity, and  $r$  is the radius of the molecule.

Determination of association constants using DOSY provides an additional NMR based method and an alternative of the classical chemical shifts titration method, particularly convenient for evidence of binding between differently sized species.<sup>14</sup> The association constant  $K_a$  for a complex of  $n$  molecule host and  $m$  molecule guest, for example,



Could be deduced from Eq. 2:

$$K_a = \frac{[C]}{[H]^n[G]^m} = \frac{[C]}{([H]_0 - n[C])^n([G]_0 - m[C])^m} \quad (3)$$

where  $[G]_0$  and  $[H]_0$  are the total concentration of the guest and host, respectively, and  $[G]$ ,  $[H]$ , and  $[C]$  the equilibrium concentrations of the free host (H), of the free guest (G), and of the complex (C). Usually the stoichiometry, that is, the values of  $n$  and  $m$ , was determined first, for example, from Job plots. The association constant is determined using Eq. 4 if the mole fraction  $\chi_b$  of the bound species is known.

$$K_a = \frac{\chi_b}{(1 - \chi_b)([H]_0 - \chi_b[G]_0)} \quad (4)$$

The diffusion coefficient observed ( $D_{obs}$ ) in the NMR experiment (fast-exchange condition) is the weighted average of the diffusion coefficient of bound ( $D_{bound}$ ) and free ( $D_{free}$ ) guest:

$$D_{obs} = \chi D_{bound} + (1 - \chi)D_{free} \quad (5)$$

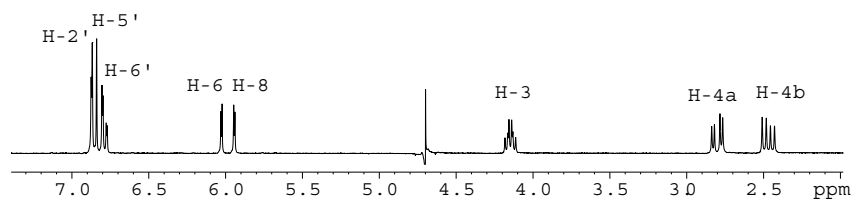


Figure 2.  $^1\text{H}$  NMR spectra of (+)catechin in  $\text{D}_2\text{O}$ .

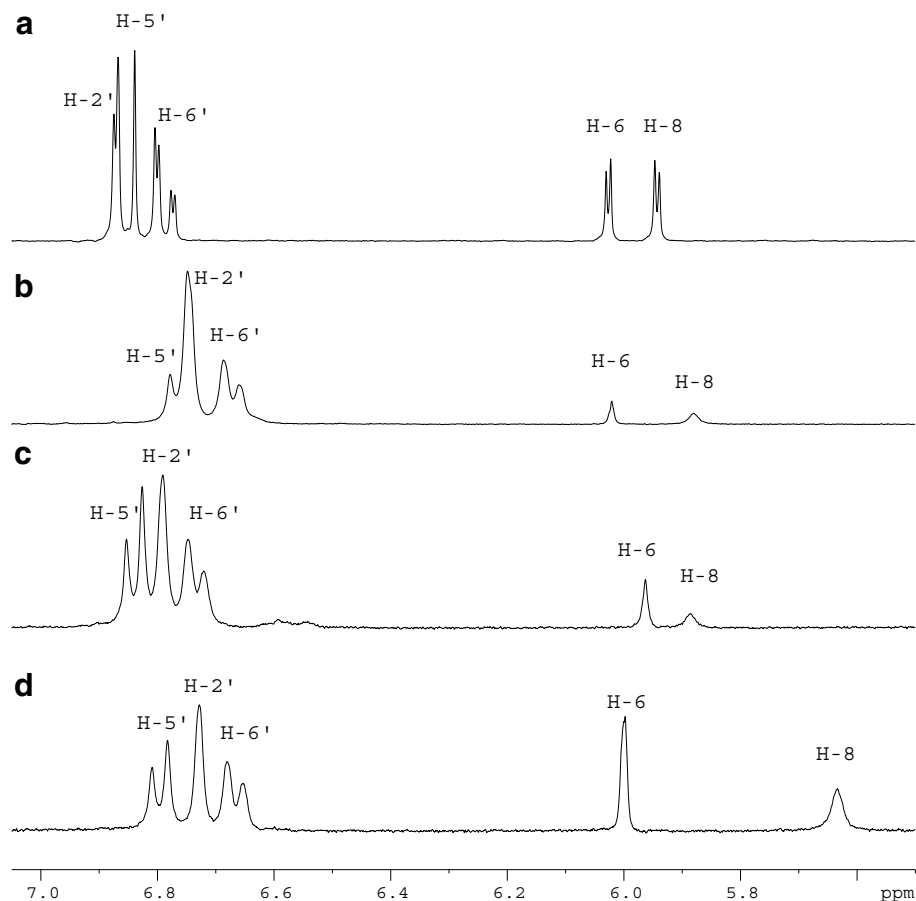


Figure 3.  $^1\text{H}$  NMR spectra: (a) CA without CDs; (b–d) inclusion complexes with  $\beta\text{-CD}$ , HP- $\beta\text{-CD}$ , and DM- $\beta\text{-CD}$ .

Table 1. The chemical shifts ( $\delta$ ) of CA,  $\beta\text{-CD}$ -, HP- $\beta\text{-CD}$ -, and DM- $\beta\text{-CD}$ -CA complexes and their complexation shifts ( $\Delta\delta$ )

	$\delta(\text{ppm})$				
	H-2'	H-5'	H-6'	H-6	H-8
CA (free)	6.87	6.85	6.79	6.03	5.94
CA- $\beta\text{-CD}$	6.75	6.76	6.67	6.02	5.88
$\Delta\delta^a$	0.12	0.09	0.11	0.01	0.06
CA-HP- $\beta\text{-CD}$	6.79	6.84	6.73	5.96	5.88
$\Delta\delta^a$	0.08	0.01	0.05	0.06	0.06
CA-DM- $\beta\text{-CD}$	6.73	6.79	6.67	5.99	5.63
$\Delta\delta^a$	0.14	0.06	0.12	0.03	0.31

<sup>a</sup>  $\Delta\delta = \delta_{(\text{free})} - \delta_{(\text{complex})}$ .

Therefore, the fraction of bound guest can be determined by

$$\chi_b = \frac{(D_{\text{free}} - D_{\text{obs}})}{(D_{\text{free}} - D_{\text{bound}})} \quad (6)$$

It is noteworthy that it is possible to obtain directly the molar fraction of the bound guest by employing Eq. 6 and, hence, by using Eq. 4, the association constant by single point determinations.

The rationale behind the extraction of the bound fraction from diffusion NMR measurements is simple. The host and guest have their own diffusion coefficients in the free state that reflect their molecular weight and

shape. Whereas the guest molecules are significantly smaller than cyclodextrin, furthermore the diffusion coefficients of the bound guests were taken to be equal to the diffusion coefficient of CD, it is assumed that, for binding of a small guest molecule to a large host molecule, the diffusion coefficient of the host is not greatly perturbed and the diffusion coefficient of the host-guest complex can be assumed to be the same as that of the non-complexed host molecule.<sup>15</sup> In the case of a weak or negligible association, the diffusion coefficients of the host and the guest will remain unchanged. For any other case, assuming fast exchange on the NMR time scale, the observed (measured) diffusion coefficients ( $D_{\text{obs}}$ ) are a weighted average of the free and bound diffusion coefficients ( $D_{\text{free}}$  and  $D_{\text{bound}}$ , respectively) and can, therefore, be used to calculate the bound fraction  $\chi_b$ , as shown in Eq. 6, in the same way that chemical shifts are used. The precise determination of the association constant implies that the stoichiometry of the interaction process is unambiguously determined. Determination of the stoichiometry of the complexes was performed using the continuous variation method (Job's method). The continuous variation analysis was applied using the H-2' proton signal of CA. The stoichiometry of the three complexes was found to be the same for all three CD utilized, as shown in Figure 4, where there is a turning point at  $r = 0.5$ , which leads to a consistent conclusion that the molar ratio between CA and the CDs utilized is 1:1.

In 2D DOSY spectra (Fig. 5) the F2 dimension shows chemical shift and F1 dimension represents self-diffusion coefficient ( $D$ ). Therefore, groups belonging to a same molecule will appear in almost the same F1 row. By using Eq. 6 and the diffusion coefficients of the free compounds reported in Table 2, we calculated a molar fraction of bound CA equal to 0.85 for the CA- $\beta$ -CD complex, which corresponded to an association constant of  $21,800 \text{ M}^{-1}$  with a complexation stoichiometry of 1:1. The same procedure applied to HP- and DM- $\beta$ -CD

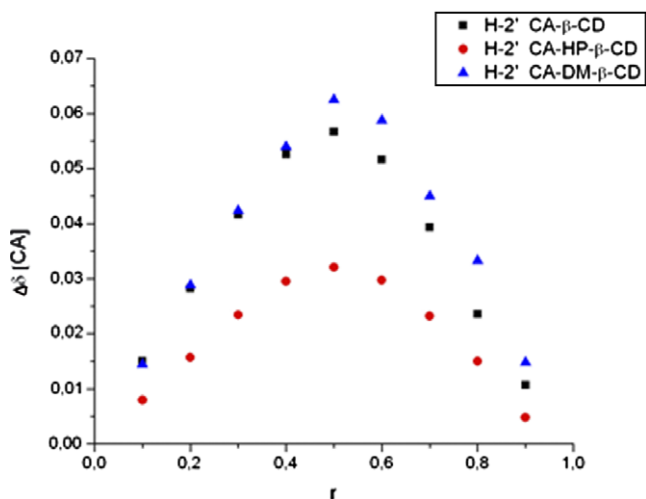


**Figure 4.** Continuous variation plot of CA- $\beta$ -CD, CA-HP- $\beta$ -CD, and CA-DM- $\beta$ -CD, showing the observed chemical shifts of H-2' of CA as a function of mole fraction.

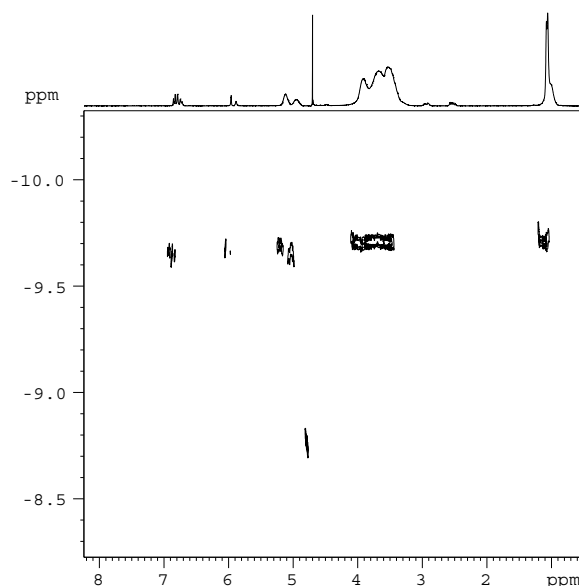


**Figure 5.** Representative DOSY spectra of CA-HP- $\beta$ -CD.

**Table 2.** Diffusion coefficients of cyclodextrins ( $D_{\text{bound}}$ ), CA in a complex form ( $D_{\text{obs}}$ ), in the free state ( $D_{\text{free}}$ ) and association constants ( $K_a$ ) at 298 K

	$D_{\text{bound}}$ ( $\text{m}^2/\text{s}$ )	$D_{\text{free}}$ ( $\text{m}^2/\text{s}$ )	$D_{\text{obs}}$ ( $\text{m}^2/\text{s}$ )	$K_a$ ( $\text{M}^{-1}$ )
CA- $\beta$ -CD	$2.420 \times 10^{-10}$	$4.04 \times 10^{-10}$	$2.63 \times 10^{-10}$	21,800
CA-HP- $\beta$ -CD	$2.125 \times 10^{-10}$	$4.04 \times 10^{-10}$	$2.51 \times 10^{-10}$	13,580
CA-DM- $\beta$ -CD	$2.278 \times 10^{-10}$	$4.04 \times 10^{-10}$	$2.66 \times 10^{-10}$	3500

gave, by single point determinations, association constants of  $13,580$  and  $3500 \text{ M}^{-1}$ , respectively (Table 2).

Further information about the inclusion mode of CA in the several CDs included in this study can be directly inferred from the 1D NMR spectra. The induced shielding of all the B-ring protons of CA suggests that this ring is inserted in the CD cavity. More direct indications concerning the geometry of the inclusion complexes can be derived from the evidence of spatial proximities between protons of CDs and CA. Figure 6 shows a partial contour plot of 2D-ROESY spectra of the inclusion complex of CA and  $\beta$ -CD. There are several intermolecular cross-peaks between H-2', H-6', and H-5' (less intense) of CA with H-5 of  $\beta$ -CD, with additional relation between H-2' of CA and H-3 of  $\beta$ -CD. However, no cross-peaks appear between the protons of the A- and C-ring and the protons of  $\beta$ -CD. This might indicate that the B-ring is deeply inserted into the cavity by the larger rim of the truncated cone. To attribute unambiguously the protons H-3, H-5, and H-6 of the cyclodextrin region, a HSQC spectrum of CA-HP- $\beta$ -CD system was performed in the same conditions as those used for the ROESY spectrum. The ROESY spectrum of the CA-HP- $\beta$ -CD complex (Fig. 7) shows correlations between H-2' of CA and H-3 and H-5 (less intense) of the CD. Also we observed an interaction between H-6 of the A-ring with H-5 of HP- $\beta$ -CD.

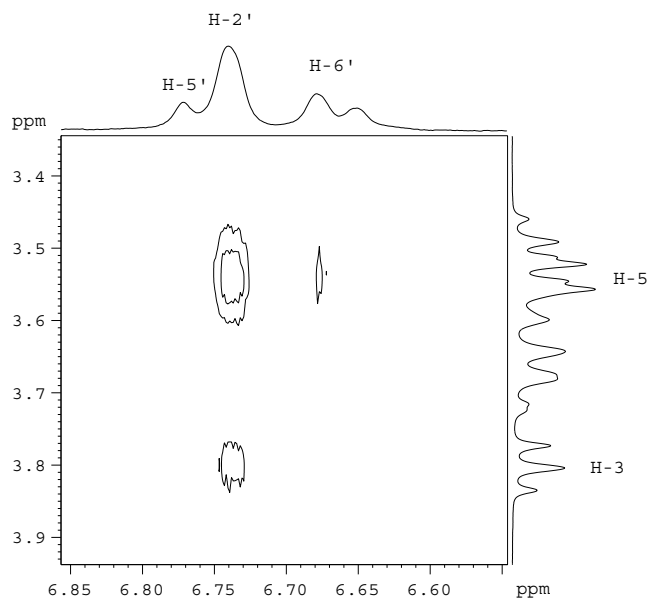


**Figure 6.** Partial contour plot of the two-dimensional ROESY spectrum of (+)catechin in presence of  $\beta$ -CD complex in  $D_2O$  (3 mM, 1:1 molar ratio).

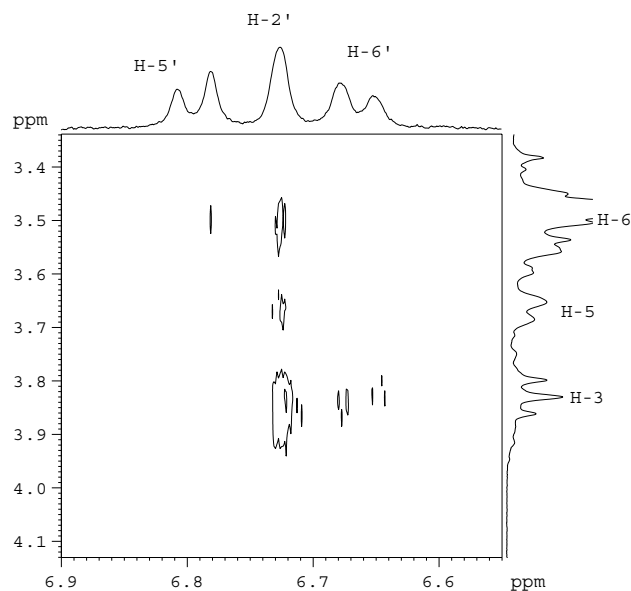


**Figure 8.** Partial contour plot of the two-dimensional ROESY spectrum of (+)catechin in presence of DM  $\beta$ -CD complex in  $D_2O$  (3 mM, 1:1 molar ratio).

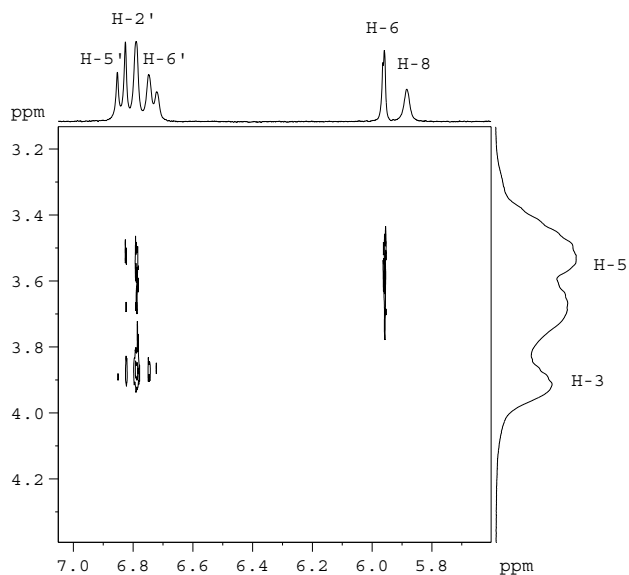


**Figure 7.** Partial contour plot of the two-dimensional ROESY spectrum of (+)catechin in presence of HP  $\beta$ -CD complex in  $D_2O$  (3 mM, 1:1 molar ratio).

CA-DM- $\beta$ -CD complex (Fig. 8) showed the same correlations between the internal H-3 and H-5 protons as those obtained with the HP- $\beta$ -CD. The analysis of the dipolar interactions generated by the internal protons of the three cyclodextrins not only confirmed some features already evidenced by the analysis of the complexation shifts, but also revealed some additional aspects. As a matter of fact, H-5 protons of  $\beta$ -CD produced remarkable crosspeak on catechin B-ring which could suggest that CA is deeply inserted into the cavity and the A-ring is oriented toward the secondary hydroxyl group of the  $\beta$ -CD, which is in agreement with the result

reported by Ishizu<sup>10</sup> and Kriz<sup>16</sup>. Figure 7 shows a contour plot of a section of the ROESY spectrum of CA and HP- $\beta$ -CD complexes. The bidimensional spectrum shows several intermolecular cross-peaks which clearly suggest that the protons of the B-ring are on the secondary face and the A-ring is on the primary face of HP- $\beta$ -CD. So, it seems that there are two models between CA and CDs.

In order to rationalize the NMR experimental results described above, we carried out molecular modeling studies of the complexes. These studies revealed that a preferred final relative orientation for all the complexes study occurs in spite of the different initial configurations arbitrarily imposed. The minimum energy complexes obtained for the three CDs under studied are shown in Figures 9–11. It is interesting to note that although no fixed distances were imposed during the docking calculations, the results are in very good agreement with the distances obtained by 2D ROESY spectra. All these complexes were further refined using a semiempirical methodology such as PM3. Noticeable differences between the  $\beta$ -CD and its derivatized forms can be observed, being the orientation of the ligand once inside of the host molecule the most relevant. A detailed description of the principal topological aspects of these complexes is discussed below.

In the case of CA- $\beta$ -CD complex, the conformation obtained by molecular modeling was in agreement with the ROESY results. The complex has the B-ring of CA oriented toward the primary rim, while both A and C rings remain oriented to the secondary rim, in such a way that the plane formed by the A-ring is placed in a  $45^\circ$  angle with respect to the plane formed by the glycosidic oxygens of the  $\beta$ -CD subunits (Fig. 12). On the other hand, it is possible to observe from Figure 9 that the A-ring of



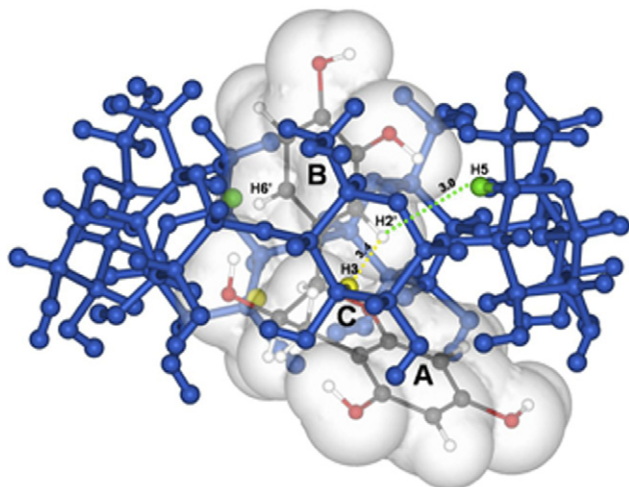


**Figure 9.** Inclusion complex between CA and  $\beta$ -CD obtained from molecular docking studies. The B-ring of CA is found inside the  $\beta$ -CD cavity, where the H-2' remains nearer to H-5 than H-3.

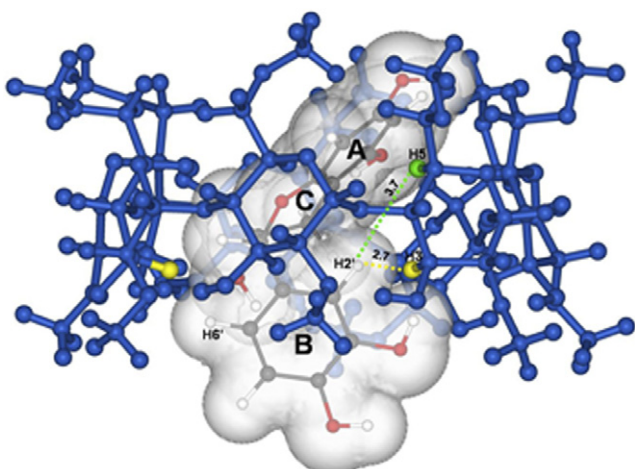


**Figure 10.** Inclusion complex between CA and DM- $\beta$ -CD obtained from molecular docking studies. The A- and C-rings are almost completely inserted on the interior of the CD, while the B-ring is mainly exposed to the outside.

CA protrudes outside of the  $\beta$ -CD, leaning closer to the secondary rim, where the H-8 of this ring remains at a reasonable distance from H-3, while the H-6 points completely out of the  $\beta$ -CD.

The theoretical results obtained from the CA-DM- $\beta$ -CD complex indicate that the B-ring of CA is oriented to the secondary rim, resulting in a complex where the CA is located in opposite direction with respect to the previous CA- $\beta$ -CD complex (Fig. 10). From the ROESY spectrum of DM- $\beta$ -CD we infer that the H-2' of CA is closer to H-3 than H-5 of the DM- $\beta$ -CD and by molecular modeling the distances are 2.7 and 3.7 Å, respectively. The A-ring of the CA is oriented in an angle near to 45° (315° if we take as a 0° reference angle the same of the  $\beta$ -CD-CA complex) with respect to the plane formed by the glycoside oxygen of the glucopyranoses. It is worth to mention that in this complex, both the

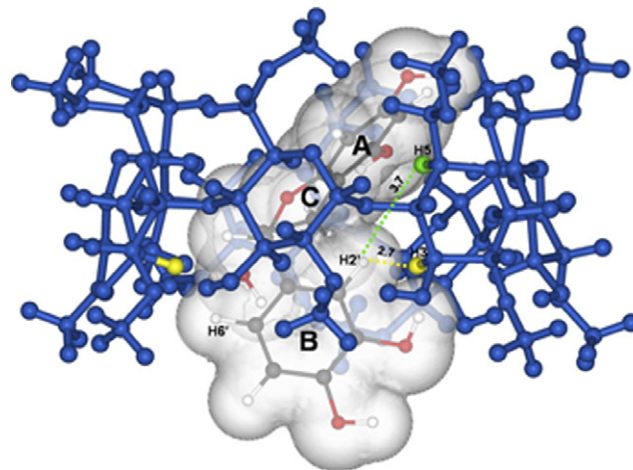


**Figure 11.** Inclusion complex between CA and HP- $\beta$ -CD obtained from molecular docking studies. The A- and C-rings are almost completely inserted on the interior of the CD, while the B-ring is mainly exposed to the outside.

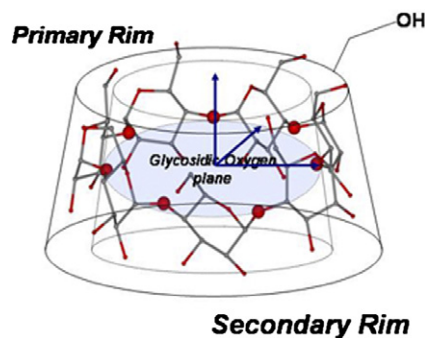


**Figure 12.** Plane formed by the glycosidic oxygen of the  $\beta$ -cyclodextrin unit.

A- and C-rings are almost completely inserted on the interior of the DM- $\beta$ -CD, while the B-ring is mainly exposed to the outside. This is in agreement with the observed differences in the cross peak of the 2D-ROESY spectra for H-2' of the CA with H-3 and H-5 for the  $\beta$ -CD and DM- $\beta$ -CD. This evidence could indicate that the B-ring of CA in the DM- $\beta$ -CD is not as deep as compared to  $\beta$ -CD. The large shielding observed in the  $^1\text{H}$  NMR spectra for the H-8 of the A-ring of CA-DM- $\beta$ -CD might be due to its close proximity to two methylenic protons (C-6) and to two H-5 of different glucopyranose subunits according to our model results.

When the ROESY spectrum of CA-HP- $\beta$ -CD is compared with that of CA-DM- $\beta$ -CD complex, it can be observed that the H-2' of the B-ring from the CA is closer to H-3 than to H-5 of the HP- $\beta$ -CD. The H-5' and the H-6' of B-ring of CA remain in the proximity of other H-3 of HP- $\beta$ -CD (Fig. 11). The B-ring of the CA remains oriented to the secondary rim, again with an angle of 45° (315°) with respect to the plane formed by the glycosidic oxygens of the HP- $\beta$ -CD. In this complex, just like in the previously described case, the B-ring of the CA is mainly located outside of the host. As a consequence of this, the model shows that both A- and C-

rings are completely inside of the hydrophobic core of the HP- $\beta$ -CD, leaving the H-6 and H-8 of the A-ring near to H-3 and H-5 of the subunits of HP- $\beta$ -CD.

The NMR experiment confirmed that CA formed 1:1 inclusion complexes with  $\beta$ -, DM- $\beta$ - and HP- $\beta$ -CD in aqueous medium. The formation constants obtained by diffusion-ordered spectroscopy (DOSY) techniques indicated the following trend upon complex formation:  $\beta$ -CD > HP- $\beta$ -CD > DM- $\beta$ -CD; which indicates that the substituents on  $\beta$ -CD hinder the inclusion of CA into the CD cavity playing an important role in the formation of the inclusion complexes. By means of experimental and theoretical methods, the present work unambiguously determined the geometrical inclusion parameters of CA on the different CDs. Besides the ROESY experiments showed that the inclusion of CA in  $\beta$ -CD has a different trend when it is compared with HP- and DM- $\beta$ -CD. These results were corroborated by molecular modeling calculations.

### 3. Experimental

#### 3.1. Materials

The (+)catechin,  $\beta$ -cyclodextrin, 2-hydroxypropyl- $\beta$ -cyclodextrin (HP- $\beta$ -CD)[M.S. = 1], and Heptakis(2,6-di-*O*-methyl)  $\beta$ -cyclodextrin (DM- $\beta$ -CD) were purchased from Sigma–Aldrich Inc. St. Louis, MO.

#### 3.2. Measurements

All NMR experiments have been performed on a Bruker AVANCE DRX300 spectrometer equipped with a pulse gradient unit capable of producing magnetic field pulse gradients in the *z*-direction of  $53.5 \text{ G cm}^{-1}$ . The spectra have been acquired in an inverted probe-head at 298 K in 5 mm tubes. All chemical shifts were relative to the DOH signal at 4.70 ppm. The NMR measurements have been done with standard BRUKER pulse sequences. Intermolecular proximity has been derived from 2D ROESY experiments. The measuring conditions for the 2D spectra were: spectral width 3000 Hz; data size 16 K/8 K; relaxation delay 2 s, and 32 scans with a mixing time of 400 ms. Phase sensitive spectra were acquired using TPPI scheme. DOSY experiments have been performed using bipolar longitudinal eddy current delay (BPLED—bipolar pulsed field gradient longitudinal eddy delay) pulse sequence.<sup>17</sup> The duration of the magnetic field pulse gradients was 3 ms with 5 ms eddy current delay and spoil gradients of 1 ms with 17:13% ratio. The pulse gradients have been incremented from 2% to 95% of the maximum gradient strength in a linear ramp.

#### 3.3. Preparation of (+)catechin-CDs complex

Inclusion complexes were obtained by mixing appropriate amounts of CA and CDs in D<sub>2</sub>O with a molar ratio of 1:1. The resulting mixture was equilibrated in a Julabo thermostatic shaking water bath for 24 h at 30 °C after which the equilibrium was reached.

The Job's plots<sup>18</sup> (i.e., continuous variation method) were determined from <sup>1</sup>H NMR data obtained in unbuffered D<sub>2</sub>O. The total molar concentration (i.e., the combined concentration of CA and CDs) was kept constant (3 mM), but the mole fraction of catechin (i.e.,  $[\text{CA}] / ([\text{CA}] + [\text{CD}])$ ) varied from 0.1 to 0.9.

#### 3.4. Molecular modeling

In silico build-up of  $\beta$ -CD, DM- $\beta$ -CD, and HP- $\beta$ -CD was carried out using the Builder module of the *InsightII* program<sup>19</sup> by adding to  $\beta$ -CD 14 methyl in position 2 and 6 (DM- $\beta$ -CD) and 7 hydroxypropyl groups (HP- $\beta$ -CD). The obtained models were subjected to optimization using a protocol of 300 steps of conjugate gradients to avoid steric hindrance and clashes that can appear in the building process. The CA was built using *Gaussview* and then it was optimized using a semiempirical method such as PM3 as implemented in *Gaussian98* package of programs.<sup>20</sup>

Autodock3.0.5<sup>21</sup> with Lamarkian Genetic Algorithm (LGA) was used to generate the starting complexes. The parameters used for the global search were an initial population of 50 individuals, with a maximal number of energy evaluations of 1,500,000 and a maximal number of generations of 50,000 as an end criterion. An elitism value of 1 was used, and a probability of mutation and crossing-over of 0.02 and 0.08 was used, respectively. From the best solutions obtained according to these parameters, some of them defined by the user as the best probabilities in our case 0.06 were further refined by a local search method such as pseudo Solis and Wets 'PSW'.

Autodock defines the conformational space implementing grids all over the space of the possible solutions. With the aim of testing the ability of Autodock to converge into solutions that are inside of the  $\beta$ -CD, a grid of 80 Å by side and 0.3 Å spacing between each point was set up in such a way that it covered both the external surface and the internal cavity of the  $\beta$ -CD.

The following procedure was employed on the  $\beta$ -CD docking simulations: 250 runs were done for each  $\beta$ -CD. At the end of each run, the solutions were separated into clusters according to their lowest RMSD and the best score value based on a free empiric energy function. Cluster solutions whose average score was not over 1 kcal mol<sup>-1</sup> with respect to the best energy obtained in the respective run were selected. Then, the solution that represents most of the complexes obtained in the run was compared with the NMR experimental data, assuring that this solution is able to represent it accurately. The selected final complexes were optimized using the semiempirical PM3 method as a refining procedure with *Gaussian98*.

#### Acknowledgments

C.J. thanks financial support of Departamento de Posgrado y Postitulo PG/57/2005 of University of Chile.

S.M. thanks Beca Memoria de Titulo de Pregrado, Chemical and Pharmaceutical Science Faculty, University of Chile. G.Z. thanks Proyecto Bicentenario de Inserción Académica CONICYT 2005. The authors are grateful to CEPEDeq from UCH for the use of NMR.

### References and notes

1. Dalluge, J. J.; Nelson, B. C. *J. Chromatogr., A* **2000**, *881*, 411.
2. Carando, S.; Teissedre, P. L. *Basic Life Sci.* **1999**, *66*, 725.
3. Yang, C. S.; Wang, Z. Y. *J. Natl. Cancer Inst.* **1993**, *85*, 1038.
4. Stavric, B. *Clin. Biochem.* **1994**, *27*, 319.
5. Testa, B.; Perrisoud, D. In *Liver Drugs: From Experimental Pharmacology to Therapeutic Applications*; CRC Press: Boca Raton, FL, 1988.
6. Atwood, J. L.; Davies, J. E. D.; Macnicol, D. D.; Vögtle, F.. In *Comprehensive Supramolecular Chemistry*; Pergamon Press: UK, 1996; Vol. 3.
7. Loftsson, L.; Brewster, M. E. *J. Pharm. Sci.* **1996**, *85*, 1017.
8. Jullian, C.; Moyano, L.; Yañez, C.; Olea-Azar, C. *Spectrochim. Acta A* **2006**, doi:10.1016/j.saa.2006.07.006.
9. Jullian, C.; Orosteguis, T.; Olea-Azar, C. *Spectrochim. Acta A*, submitted for publication.
10. Ishizu, T.; Kintsu, K.; Yamamoto, H. *J. Phys. Chem. B* **1999**, *103*, 8992.
11. Fielding, L. *Tetrahedron* **2000**, *56*, 6151.
12. Cameron, K.; Fielding, L. *J. Org. Chem.* **2001**, *66*, 6891.
13. Laverde, A., Jr.; da Conceição, G. J. A.; Queiroz, S. C. N.; Fujiwara, F. Y.; Marsaioli, A. J. *Magn. Reson. Chem.* **2002**, *40*, 433.
14. Cameron, K. S.; Fielding, L. *Magn. Reson. Chem.* **2002**, *40*, S106.
15. Wimmer, R.; Aachmann, F. L.; Larsen, K. L.; Petersen, S. B. *Carbohydr. Res.* **2002**, *337*, 841.
16. Kriz, Z.; Koca, J.; Imberty, A.; Charlot, A.; Auzely-Velty, R. *Org. Biomol. Chem.* **2003**, *1*, 2590–2595.
17. Wu, D.; Chen, A.; Johnson, C. S. *J. Magn. Reson., Ser A* **1995**, *115*, 260.
18. Job, P. *Ann. Chim.* **1928**, *9*, 113.
19. InsightII, MSI, San Diego, California.
20. Frisch, M. J.; Trucks, G. W.; Schlegel, H. B.; Scuseria, G. E.; Robb, M. A.; Cheeseman, J. R.; Zakrzewski, V. G.; Montgomery, J. A.; Stratmann, R. E.; Burant, J. C.; Dapprich, S.; Millam, J. M.; Daniels, A. D.; Kudin, K. N.; Strain, M. C.; Farkas, O.; Tomasi, J.; Barone, V.; Cossi, M.; Cammi, R.; Mennucci, B.; Pomelli, C.; Adamo, C.; Clifford, S.; Ochterski, J.; Petersson, G. A.; Ayala, P. Y.; Cui, Q.; Morokuma, K.; Malick, D. K.; Rabuck, A. D.; Raghavachari, K.; Foresman, J. B.; Cioslowski, J.; Ortiz, J. V.; Stefanov, B. B.; Liu, G.; Liashenko, A.; Piskorz, P.; Komaromi, I.; Gomperts, R.; Martin R. L.; Fox, D. J.; Keith, T.; Al-Laham, M. A.; Peng, C. Y.; Nanayakkara, A.; Gonzalez, C.; Challacombe, M.; Gill, P. M. W.; Johnson, B. G.; Chen, W.; Wong, M. W.; Andres, J. L.; Head-Gordon, M.; Replogle, E. S.; Pople, J. A. Gaussian 98 (revision a.7), Gaussian, Inc., Pittsburg, PA, 1998.
21. Morris, G. M.; Goodsell, D. S.; Halliday, R. S.; Huey, R.; Hart, W. E.; Belew, R. K.; Olson, A. J. *J. Comput. Chem.* **1998**, *19*, 1639.